Chirality

Deutsche Ausgabe: DOI: 10.1002/ange.201507590
Internationale Ausgabe: DOI: 10.1002/anie.201507590

Disappearing Enantiomorphs: Single Handedness in Racemate Crystals

*Manfred Parschau and Karl-Heinz Ernst**

Abstract: *Although crystallization is the most important method for the separation of enantiomers of chiral molecules in the chemical industry, the chiral recognition involved in this process is poorly understood at the molecular level. We report on the initial steps in the formation of layered racemate crystals from a racemic mixture, as observed by STM at submolecular resolution. Grown on a copper single-crystal surface, the chiral hydrocarbon heptahelicene formed chiral racemic lattice structures within the first layer. In the second layer, enantiomerically pure domains were observed, underneath which the first layer contained exclusively the other enantiomer. Hence, the system changed from a 2D racemate into a 3D racemate with enantiomerically pure layers after exceeding monolayer-saturation coverage. A chiral bias in form of a small enantiomeric excess suppressed the crystallization of one double-layer enantiomorph so that the pure minor enantiomer crystallized only in the second layer.*

Optical resolution—the separation of chiral compounds into their enantiomers through crystallization—is the most important means in the chemical industry for obtaining enantiomerically pure compounds useful as pharmaceuticals, flagrances, pesticides, herbicides, and flavors.[1,2] This method dates back to 1848, when Pasteur obtained a conglomerate of homochiral crystals upon crystallizing the ammonium sodium salt of "acide racemique", namely, racemic tartaric acid.[3] To date, the molecular mechanism of this resolution phenomenon is not understood.[4] In particular, it is unclear why the majority of chiral molecules crystallize into racemic (*rac*) compounds, that is, a single crystal is composed of pairs of both enantiomers, instead of forming conglomerates.[5,6] In 1895, the mineralogist Liebisch provided an explanation by reporting for eight samples that the enantiomers are more densely packed in their racemic crystals than in homochiral crystals.[7] Although confirmed for many compounds,[6] the "Liebisch rule" does not apply to amino acids.[8]

Under special conditions, spontaneous symmetry breaking in crystallization experiments has led to the formation of only one crystal enantiomorph in the precipitate.[9] If there is no chiral bias, both enantiomorphs are observed with equal probability when the experiment is repeated. If a chiral bias exists, however, enantioselectivity is possible.[10] An interesting mirror-symmetry-breaking effect in crystallization is induced by chiral additives in achiral crystals, thus leading to helicoidal deformation during crystal growth.[11] In another example from polymer chemistry, the transmission of chirality from side chains, either as the result of a small concentration of chiral side chains or an enantiomeric excess in the side chains, into a single sense of helicity has been reported for helical polyisocyanate polymers.[12,13] These modes of chiral amplification have been termed the "sergeants-and-soldiers" principle and the "majority rule", respectively. The first 2D analogues of the "sergeants-and-soldiers" and "majority-rule" effects were reported by us after doping succinic acid and *meso*-tartaric acid monolayers on Cu(110) with chiral tartaric acid,[14] and for enantiomorphous domains of racemic heptahelicene on Cu(111) at small *ee* values, respectively.[15]

As one kind of manifestation of chirality,[16] molecular helicity plays a fundamental role in molecular biology.[17] It also has implications in devices based on organic materials, such as molecular-spin filters,[18] liquid crystals,[19] and circular dichroic photonics.[20] To obtain a better understanding of molecular chiral recognition, model studies on well-defined surfaces by scanning tunneling microscopy (STM) have become popular.[21] In particular, carbohelicenes,[22] *ortho*-annulated, π-conjugated aromatic hydrocarbons, have been investigated on various surfaces.[23] Herein we report the observation that a single sense of enantiomorphism can be induced in multilayered racemate crystals. The crystallization of more than one monolayer of heptahelicene ($C_{30}H_{18}$, [7]H, Figure 1) on a copper(111) surface led to the formation of mirror domains, that is, domains that are tilted to opposite directions with respect to the underlying substrate and not superimposable by rotation and translation in two dimensions. These two enantiomorphs are racemic and are composed of enantiomerically pure layers with alternating handedness. Even at small *ee* values, exclusively one enan-

[*] Dr. M. Parschau, Prof. Dr. K.-H. Ernst
Nanoscale Materials Science Laboratory
Empa, Swiss Laboratories for Materials Science and Technology
Ueberlandstrasse 129, CH-8600 Dübendorf (Switzerland)
E-mail: karl-heinz.ernst@empa.ch
Prof. Dr. K.-H. Ernst
Department of Chemistry, University of Zurich
Winterthurerstrasse 190, CH-8057 Zürich (Switzerland)

Supporting information for this article is available on the WWW under http://dx.doi.org/10.1002/anie.201507590.

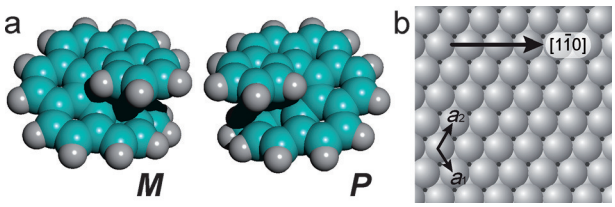

Figure 1. Space-filling models of a) *M*- and *P*-heptahelicene and b) the Cu(111) surface. Substrate vectors a_1 and a_2 and the [1$\bar{1}$0] direction are indicated.

tiomorph of these thin 3D crystals was observed. Moreover, we report herein a new phenomenon: enantiospecific dewetting of the first layer, whereby only the majority enantiomer remains in the first layer, and the second layer contains exclusively the minority enantiomer.

As soon as the coverage of [7]H on Cu(111) exceeded first-layer-saturation coverage ($\theta_{rel}=1$),[24] second-layer islands crystallized. Figure 2a shows an STM image of a sample after the deposition of 103% of the coverage of a close-packed racemic monolayer ($\theta_{rel}=1.03$) of *rac*-[7]H. Besides a second-layer island (red area), large uncovered first-layer areas are observed (gray areas). Many short segments of zigzag rows can be identified in the uncovered first layer. Such a motif is characteristic for the racemate, which forms from low coverages on heterochiral *M*–*P* pairs, and with increasing coverage forms *M*–*P* zigzag rows.[25] These *M*–*P* motifs of *rac*-[7]H have also been observed on other surfaces.[26] However, the usual good long-range order of the saturated monolayer (see Figure 1 in the Supporting Information) is not observed in this case. At intermediate coverages between the saturated monolayer and a completely filled second layer ($1<\theta_{rel}>1.61$, Figure 2b), the second-layer islands are actually larger than expected for a second layer just growing on the close-packed racemic first-layer saturation structure. Often second-layer islands completely cover an atomically flat terrace, whereas a depleted first layer covers the rest of the surface (see Figure 2 in the Supporting Information). Apparently, the nucleation temperature for the double-layer phase is higher than for the monolayer, and the molecules are still very mobile and travel over a large distance on the surface. The diffusion of [7]H molecules over long distances thus supports the ongoing growth of the double-layer phase and leads to the low density of the uncovered first layer. Even at a coverage of $\theta_{rel}=1.01$, the first layer was not found to be at its usual 100% coverage. When the first layer finally starts to nucleate, the temperature and coverage are too low for the formation of long-range ordered domains of zigzag rows, thus leading to the high degree of disorder at these intermediate coverages.

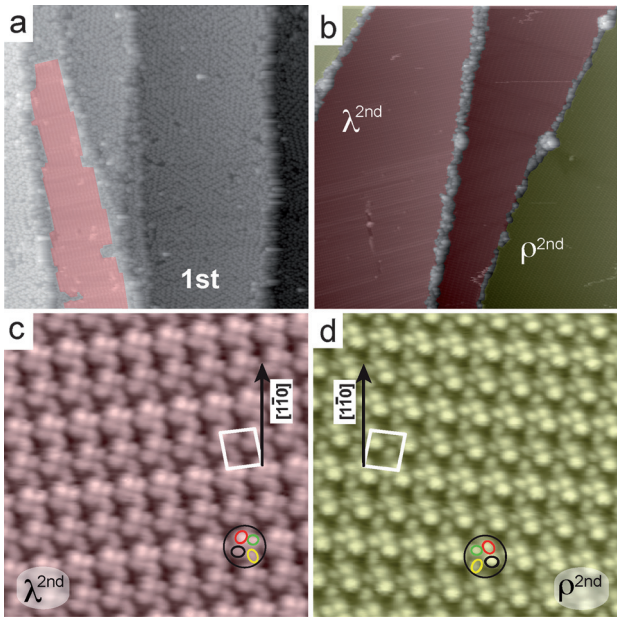

Figure 2. a) STM image of a [7]H second-layer island (colored). The gray area shows the not-well-ordered first layer (100×100 nm^2, $U=2.72$ V, $I=20$ pA, $\theta_{rel}=1.03$). b) STM image of the completely filled second layer. Mirror domains (red, green) are observed on different terraces (150×150 nm^2, $U=2.96$ V, $I=19$ pA, $\theta_{rel}=1.60$). c,d). Submolecular-resolution STM images (10×10 nm^2, $\theta_{rel}=1.7$) of both mirror domains in the second layer. All molecules of a single domain show the same distinct chiral four-lobe pattern (colored ellipses). A single domain is therefore homochiral in the second layer. The sequence of an asymmetric four-lobe appearance (red–green–yellow) has opposite sense for mirror domains and enables determination of the absolute handedness of the molecules (c: $U=-2.56$ V, $I=22$ pA; d: $U=-2.36$ V, $I=55$ pA).

By virtually counting all molecules in several STM images taken of the uncovered first layer, we deduced an average covered area per molecule of 112 ± 7 Å^2. This value is substantially larger than the covered molecular area determined for the close-packed first layer (104.4 Å^2/molecule, $\theta_{abs}\approx0.958$ molecules/nm^2).[25b] From STM and low-energy electron diffraction (LEED) studies, the second-layer periodicity was found to be $(2\,5,\ -5\ -1)$ with respect to the Cu(111) surface periodicity (see Figure 3 in the Supporting Information),[27] which means that one [7]H molecule occupies an area equivalent to 23 Cu(111) surface atoms, that is, 129.6 Å^2 ($\theta_{abs}\approx0.772$ molecules/nm^2). A completely filled second layer is observed at a relative coverage of $\theta_{rel}=1.60$ (Figure 2b). From this experimental value and the determined lateral densities of the saturated monolayer and second layer, it follows unambiguously that the density of the first layer underneath the second-layer island must be identical to that of the second layer (2×0.772 nm^{-2}/0.958 nm$^{-2}=1.61$). This conclusion was confirmed by LEED, which showed a periodicity of the double-layer system that is identical to the periodicity observed for the second layer by STM (Figure 2c,d). Hence, there is no lattice mismatch between the first and the second layer. The absence of Moiré patterns in the second-layer STM images supports this conclusion. However, we note that along one adlattice vector ($b_2\approx[1\bar{1}0]\pm10.9°$; see Figure 3 in the Supporting Information), the molecules of every second row appear somewhat brighter by STM (Figure 2c), possibly owing to a slight buckling of the second layer.

STM images with submolecular resolution also revealed that the second-layer domains were homochiral (Figure 2c,d). Each second-layer molecule appeared as an asymmetric four-lobe pattern; and all patterns in a single domain showed identical handedness. This result is in stark contrast to the domain composition of the racemic first layer, in which an alternating mirrorlike STM appearance of [7]H molecules in single domains was observed (see Figure 1 in the Supporting Information).[15] To determine which mirror domain contained which enantiomer in the second layer, we performed a control experiment with a double layer of *M*-[7]H (Figure 3a). Although the pure-enantiomer double-layer symmetry was hexagonal instead of oblique for the second-layer racemic structure,[28] the STM contrast for a single molecule

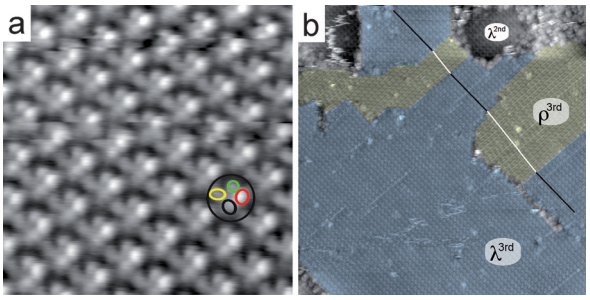

Figure 3. a) STM image (8.5×8.5 nm^2, $U=2.35$ V, $I=40$ pA, $\theta_{rel}=1.92$) of the second layer after the deposition of enantiomerically pure *M*-[7]H. The four-lobe STM contrast of a single molecule (red–green–yellow) runs counterclockwise for *M*-[7]H. b) STM image (67×67 nm^2, $U=2.24$ V, $I=21$ pA, $\theta_{rel}=2.3$) of the third layer. Mirror domains are only slightly azimuthally misaligned with respect to one another, as indicated by white and black lines.

was again characterized by the distinctive four-lobe pattern. Its handedness was identical to that of the molecules in the ρ^{2nd} layer, that is, the lobe sequence (red–green–yellow) runs counterclockwise. Thus, *P* enantiomers are in the second layer of the λ domains (λ^{2nd}), and *M* enantiomers are in the second layer of the ρ domains (ρ^{2nd}). This structure is in contrast to the multilayer structure of chiral rubrene, for which racemic mirror domains were reported for the top layer.[29]

As in the case of the *rac*-[7]H monolayer (see Figure 1 in the Supporting Information), the second-layer mirror domains showed opposite tilt angles of ±10.9° with respect to the high-symmetry [1$\bar{1}$0] direction of the Cu surface lattice. Whereas perfect wetting of the first layer by the second layer was observed, more layers appeared with increasing coverage that did not completely cover the second layer. That is, the fourth layer appeared before the second layer was completely covered by the third layer. In an STM image of a sample with a large third-layer island (Figure 3b), two domains with enantiomerically pure top layers, colored blue and yellow, were identified. Because the alignment is identical to that of λ^{2nd} (gray), we assume that λ^{3rd} (blue) grows on top of λ^{2nd}. Only *M*-[7]H molecules were located in the third layer of this domain (see Figure 4a in the Supporting Information). If no further rearrangement in the multilayered samples occurred, the enantiomeric layer sequence must then be *M*–*P*–*M* in this domain. Even the fourth layer of a single domain was homochiral (see Figure 4b in the Supporting Information). However, we note that the third-layer mirror domains showed only a small difference in azimuthal alignment (Figure 3b), instead of the 22° angle (i.e. 2 × 10.9°) observed for the mirror domains of the first and second layers.

Experiments with *rac*-[7]H do not provide unambiguously the answer to the question whether the double layer is homochiral or racemic, or whether it has a racemic first layer with a homochiral layer on top. This information, however, was clearly derived from experiments on samples with an enantiomeric excess. Such samples showed a single enantiomorphism for all second-layer islands. These samples contained exclusively the minor enantiomer in the second layer. Figure 4a shows a large second-layer domain (red area) formed at 7% *ee* and $\theta_{rel}=1.05$ (105% of the nominal coverage for the close-packed racemic monolayer). This STM image shows an area of 2.62 μm^2! The second-layer domain is not limited to a single terrace, but extends over a monoatomic step onto another terrace (Figure 4a, bottom). Figure 4b shows the same domain at larger magnification (area of 0.16 μm^2), which reveals the lower degree of order in the first layer with respect to the second layer. In the racemic samples, double-layer nucleation and growth seemed strongly favored, so that a single double-layer island and large [7]H-depleted first-layer areas were formed. When an excess of *M*-[7]H was present, only λ^{2nd} domains were observed, whereas with an excess of *P*-[7]H, only ρ^{2nd} domains were present (Figures 4c,d). If the homochiral content of the second layer is taken into account, this result indicates that only the minority enantiomer is found in the second layer for samples containing one enantiomer in excess.[30]

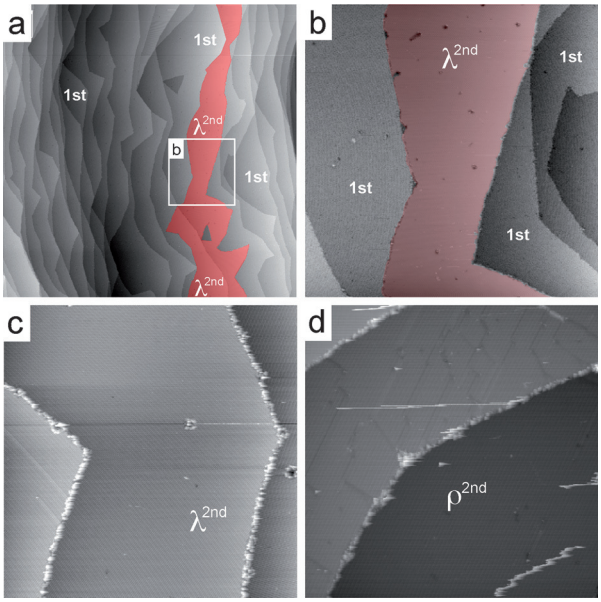

Figure 4. The formation of single enantiomorphs in the presence of an enantiomeric excess. a,b) Long-range STM images (1620×1620 nm^2 and 400×400 nm^2, $U=2.67$ V, $I=25$ pA, $\theta_{rel}=1.05$, 7% *ee*). Only one large second-layer domain with *P*-[7]H molecules in the second layer is observed (red area). A step edge of the substrate runs through the second-layer domain (a, bottom). The area of STM image (b) is shown by a square in (a). c) STM image (200×200 nm^2, $U=2.89$ V, $I=16$ pA, $\theta=1.60$, 8% *ee*) of a double-layer sample with exclusively *P*-[7]H in the second layer. d) STM image of a double layer at a negative *ee* value, with the second layer consisting of *M*-[7]H molecules (200×200 nm^2, $U=3.02$ V, $I=14$ pA, $\theta=1.61$, 8% *ee*).

A completely filled homochiral top layer was formed by samples with small *ee* values at the corresponding coverage ($\theta_{rel}=1.60$, Figure 4c,d). Because the composition of such samples is still close to racemic, the other enantiomer must be in the first layer.[30] This conclusion was confirmed by the following experiment: When a coverage of $\theta_{rel}=0.9$ of the racemate plus $\theta_{rel}=0.6$ of *M*-[7]H is established (40% *ee*), the relative coverage of *P*-[7]H is then $\theta_{rel}=0.45$. Assuming that all *P*-[7]H molecules are indeed in the second layer, 55.9% of

the surface area must show second-layer islands ($0.45 \times 129.6 \times 1/104.4 \times 100 = 55.9$), whereas in the case that the covered first layer is racemic, only two thirds of *P*-[7]H would be in the top layer, thus corresponding to 37.2 % of the surface area. The evaluation of an area of 0.55 μm^2 (i.e. 25 STM images, each $138 \times 159\ nm^2$) revealed that 56.5 % of the surface was covered by second-layer islands. Under such conditions, the uncovered first layer shows patterns that have been reported for pure *M*-[7]H (see Figure 5 in the Supporting Information).[31] Hence, *P*-[7]H grows as λ^{2nd} on top of an enantiomerically pure *M*-[7]H first layer (λ^{1st}), whereas the ρ mirror domain consists of an enantiomerically pure *P*-[7]H layer (ρ^{1st}) covered by a pure *M*-[7]H layer (ρ^{2nd}).

The fact that second-layer mirror domains, λ^{2nd} and ρ^{2nd}, completely cover atomically flat terraces of the substrate, indicates that mirror-domain boundaries (MDBs) are energetically unfavorable and thus rather coincide with monoatomic steps of the metal surface (Figure 2b). Such an observation was also made for mirror domains of the *rac*-[7]H monolayer.[15] When the sample had an enantiomeric excess, one of the racemic mirror domains was suppressed owing to a chiral bias of the excess at the domain edge in combination with the tendency to avoid energetically less favored MDBs.[15] A similar effect was observed in this study for the double-layer system, with the separation of enantiomers into alternate 2D homochiral layers. The chiral bias at the boundary between the area containing one of the enantiomers in excess and the homochiral first layer of λ or ρ domains decides not only the preferred orientation (as for the *rac*-[7]H monolayer), but also which enantiomer can nucleate in the first layer. To enable the formation of double-layer domains that are as large as possible, all molecules of the minor enantiomer move to the second layer. This behavior has the unique consequence that only a single enantiomer is exposed to the medium above the surface at small *ee* values.[30]

In conclusion, although [7]H is known to crystallize into a conglomerate from solution,[32] it forms, at least in the first few layers addressable with STM, racemic crystals on Cu(111). As soon as the coverage exceeds one monolayer, double-layer nucleation and growth, with alternating enantiomerically pure layers, is preferred over the otherwise observed *M*–*P* zigzag features within the first layer. A small enantiomeric excess leads to a double-layer system with only the minority enantiomer in the top layer and the majority enantiomer in the first layer. Our results shows that chiral amplification due to an enantiomeric excess or chiral doping is not limited to monolayer systems at surfaces, but can also induce single enantiomorphism in 3D systems at mesoscopic length scales.

Experimental Section

The experiments were carried out in two different ultra-high-vacuum chambers (base pressure ca. 1×10^{-10} mbar) equipped with standard single-crystal surface-preparation equipment and a variable- or low-temperature scanning tunneling microscope (VT-STM or LT-STM). Racemic [7]H was synthesized and separated into enantiomers as described previously.[33] The absolute configuration of the enantiomers was determined by vibrational circular dichroism and theoretical modeling.[34] The [7]H molecules (racemate as well as pure enantiomers) were deposited from a home-made twin Knudsen cell by thermal evaporation onto a Cu(111) surface held at room temperature. STM images were taken after cooling of the sample to temperatures as low as 60 K (VT-STM) or 7 K (LT-STM). Samples with different *ee* values ($([M]-[P])/([M]+[P])$; i.e., positive values indicate an excess of *M*-[7]H) were obtained by evaporation, for different periods of time, either of the two pure enantiomers at identical sublimation temperatures or the racemate and the additional enantiomer ($T_{cell} = 160\,°C$). Coverage calibrations were performed relative to complete monolayer coverage of the pure enantiomers and the racemate. The relatively low evaporation temperature and the associated long evaporation times for achieving monolayer coverage led to an accuracy of coverage of less than 1 %.

Acknowledgements

Financial support from the Swiss National Science Foundation (Supramolecular Chiral Films) is gratefully acknowledged. We thank Jack D. Dunitz for fruitful discussions.

Keywords: chiral amplification · chirality · crystal growth · helicenes · scanning probe microscopy

How to cite: *Angew. Chem. Int. Ed.* **2015**, *54*, 14422–14426
Angew. Chem. **2015**, *127*, 14630–14634

[1] R. A. Sheldon in *Chiral Technologies*: *Industrial Synthesis of Optically Active Compounds*, Marcel Dekker, New York, **1993**, pp. 173–204.
[2] G. Coquerel, *Top. Curr. Chem.* **2007**, *269*, 1–51.
[3] L. Pasteur, *Ann. Chim. Phys.* **1848**, *24*, 442–459.
[4] L. Addadi, S. Weiner, *Nature* **2001**, *411*, 753–754.
[5] J. Jacques, A. Collet, S. H. Wilen, *Enantiomers*, *Racemates and Resolution*, Krieger, Malabar, **1994**.
[6] C. P. Brock, W. B. Schweitzer, J. D. Dunitz, *J. Am. Chem. Soc.* **1991**, *113*, 9811–9820.
[7] Communicated at the Sitzung der Königlichen Gesellschaft der Wissenschaften zu Göttingen, December 8, 1894. The analysis by Liebisch is mistakenly known nowadays as "Wallach's rule" (first used in Ref. [6]), because Liebisch also reported results in: O. Wallach, *Liebigs Ann. Chem.* **1895**, *286*, 119–143.
[8] J. D. Dunitz, A. Gavezzotti, *J. Phys. Chem. B* **2012**, *116*, 6740–6750.
[9] a) D. K. Kondepudi, R. J. Kaufman, N. Singh, *Science* **1990**, *250*, 975–976; b) C. Viedma, *Phys. Rev. Lett.* **2005**, *94*, 065504; c) J. M. McBride, R. L. Carter, *Angew. Chem. Int. Ed. Engl.* **1991**, *30*, 293–295; *Angew. Chem.* **1991**, *103*, 298–300; d) Y. El-Hachemi, J. Crusats, J. M. Ribo, J. M. McBride, S. Veintemillas-Verdaguer, *Angew. Chem. Int. Ed.* **2011**, *50*, 2359–2363; *Angew. Chem.* **2011**, *123*, 2407–2411.
[10] W. L. Noorduin, P. van der Asdonk, H. Meekes, W. J. P. van Enckevort, B. Kaptein, M. Leeman, R. M. Kellogg, E. Vlieg, *Angew. Chem. Int. Ed.* **2009**, *48*, 3278–3280; *Angew. Chem.* **2009**, *121*, 3328–3330.
[11] A. G. Shtukenberg, Y. O. Punin, A. Gujral, B. Kahr, *Angew. Chem. Int. Ed.* **2014**, *53*, 672–699; *Angew. Chem.* **2014**, *126*, 686–715.
[12] a) M. M. Green, M. P. Reidy, R. J. Jonson, G. Darling, D. J. O'Leary, G. Wilson, *J. Am. Chem. Soc.* **1989**, *111*, 6452–6454; b) M. M. Green, J. W. Park, T. Sato, A. Teramoto, S. Lifson, R. Selinger, J. V. Selinger, *Angew. Chem. Int. Ed.* **1999**, *38*, 3138–3154; *Angew. Chem.* **1999**, *111*, 3328–3345.
[13] M. M. Green, B. A. Garetz, B. Munoz, H. P. Chang, S. Hoke, R. G. Cooks, *J. Am. Chem. Soc.* **1995**, *117*, 4181–4182.

[14] a) M. Parschau, S. Romer, K.-H. Ernst, *J. Am. Chem. Soc.* **2004**, *126*, 15398 – 15399; b) M. Parschau, T. Kampen, K.-H. Ernst, *Chem. Phys. Lett.* **2005**, *407*, 433 – 437.
[15] R. Fasel, M. Parschau, K.-H. Ernst, *Nature* **2006**, *439*, 449 – 452.
[16] R. S. Cahn, C. Ingold, V. Prelog, *Angew. Chem. Int. Ed. Engl.* **1966**, *5*, 385 – 415; *Angew. Chem.* **1966**, *78*, 413 – 447.
[17] T. Nakano, Y. Okamoto, *Chem. Rev.* **2001**, *101*, 4013 – 4038.
[18] R. Naaman, D. H. Waldeck, *J. Phys. Chem. Lett.* **2012**, *3*, 2178 – 2187.
[19] R. P. Lemieux, *Acc. Chem. Res.* **2001**, *34*, 845 – 853.
[20] Y. Yang, R. C. da Costa, M. J. Fuchter, A. J. Campbell, *Nat. Photonics* **2013**, *7*, 634 – 638.
[21] a) K.-H. Ernst, *Phys. Status Solidi B* **2012**, *249*, 2057 – 2088; b) J. A. A. W. Elemans, I. De Cat, H. Xu, S. De Feyter, *Chem. Soc. Rev.* **2009**, *38*, 722 – 736; c) R. Raval, *Chem. Soc. Rev.* **2009**, *38*, 707 – 721.
[22] Y. Shen, C.-F. Chen, *Chem. Rev.* **2012**, *112*, 1463 – 1535.
[23] M. Gingras, *Chem. Soc. Rev.* **2013**, *42*, 1051 – 1095.
[24] We previously used $\theta = 1$ for the close-packed first layer of the pure enantiomers,[25b] which is denser than the close-packed layer of the racemate. The density of the latter is 93.7 % that of the densest enantiomerically pure monolayer.
[25] a) K.-H. Ernst, S. Baumann, C. P. Lutz, J. Seibel, L. Zoppi, A. J. Heinrich, *Nano Lett.* **2015**, *15*, 5388 – 5392; b) M. Parschau, R. Fasel, K.-H. Ernst, *Cryst. Growth Des.* **2008**, *8*, 1890 – 1896.
[26] a) J. Seibel, M. Parschau, K.-H. Ernst, *J. Phys. Chem. C* **2014**, *118*, 29135 – 29141; b) J. Seibel, M. Parschau, K.-H. Ernst, *J. Am. Chem. Soc.* **2015**, *137*, 7970 – 7973.
[27] The (2×2) transformation matrix links the molecular-adsorbate lattice vectors (b_1, b_2) to the substrate lattice vectors (a_1, a_2) according to the equations $b_1 = m^{11}a_1 + m^{12}a_2$ and $b_2 = m^{21}a_1 + m^{22}a_2$, and is written herein in the form $(m^{11}\ m^{12}, m^{21}\ m^{22})$; see: L. Merz, K.-H. Ernst, *Surf. Sci.* **2010**, *604*, 1049 – 1054.
[28] M. Parschau, U. Ellerbeck, K.-H. Ernst, *Colloids Surf. A* **2010**, *354*, 240 – 245.
[29] M. Pivetta, M.-C. Blüm, F. Patthey, W.-D. Schneider, *J Phys Chem. B* **2009**, *113*, 4578 – 4581.
[30] At sufficient *ee* values and coverage, the major enantiomer forms enantiomerically pure double layers next to the racemic double layers.
[31] R. Fasel, M. Parschau, K.-H. Ernst, *Angew. Chem. Int. Ed.* **2003**, *42*, 5178 – 5181; *Angew. Chem.* **2003**, *115*, 5336 – 5339.
[32] R. H. Martin, M. J. Marchant, *Tetrahedron* **1974**, *30*, 343 – 345.
[33] K.-H. Ernst, Y. Kuster, R. Fasel, M. Müller, U. Ellerbeck, *Chirality* **2001**, *13*, 675 – 678.
[34] T. Bürgi, A. Urakawa, B. Behzadi, K.-H. Ernst, A. Baiker, *New J. Chem.* **2004**, *28*, 332 – 334.

Received: August 13, 2015
Published online: October 6, 2015